

Origin of spontaneous magnetization reversal in exchange biased heterostructures

Zhi-Pan Li,* Casey W. Miller,† Igor V. Roshchin,‡ and Ivan K. Schuller

Physics Department, University of California, San Diego, La Jolla, California 92093-0319, USA

(Received 16 November 2006; revised manuscript received 21 May 2007; published 17 July 2007)

The dependence of thermally induced spontaneous magnetization reversal on time-dependent cooling protocols implies that this reversal is energetically favored, contrary to the prediction of existing positive exchange bias models. Slow cooling through and long waiting near the Néel temperature of the antiferromagnet enhances the magnitude of the magnetization reversal. Further, cycling the temperature around the Néel temperature leads to a thermal training effect that causes the reversal magnitude to incrementally increase to a maximum value. An extended model of exchange bias that explicitly considers domain walls forming parallel to the interfaces in either the ferromagnet or antiferromagnet is shown to predict spontaneous reversal, the sign of exchange bias, and to allow a qualitative description of the associated dynamics.

DOI: [10.1103/PhysRevB.76.014423](https://doi.org/10.1103/PhysRevB.76.014423)

PACS number(s): 75.70.-i, 75.60.Jk

I. INTRODUCTION

When a ferromagnet/antiferromagnet (FM/AF) heterostructure is cooled in a magnetic field (H_{FC}) below the Néel temperature (T_N) of the AF,¹⁻³ a phenomenon known as exchange bias (EB) causes the hysteresis loop to shift along the magnetic field axis by an amount known as the exchange bias field (H_{EB}). This phenomenon has been intensely studied in the past decade due to its significance in providing a magnetic reference in spin valve devices.⁴ More fundamentally, exchange bias is of physical importance in understanding a rich variety of phenomena in coupled magnetic materials.⁵⁻⁸

We recently demonstrated that a thin exchange biased FM layer can fully reverse its magnetization to point against a constant H_{FC} during cooling.⁹ A similar behavior has been observed in ferrimagnet Gd-Co alloys¹⁰ and Gd-Co multilayer systems,¹¹ which results from two antiferromagnetically coupled spin species competing to align with the field. In the present case, a similar competition occurs between the interfacial coupling and Zeeman energies of FM/AF heterostructures. A prerequisite for spontaneous magnetization reversal is positive exchange bias (PEB), where the hysteresis loop is shifted in the direction of H_{FC} .⁶ It is generally believed that PEB arises when H_{FC} is large enough to overcome the antiferromagnetic interfacial coupling, thus aligning uncompensated AF moments along the field. In other words, PEB requires $|E_{AF-Z}| > |E_{int}|$, where E_{AF-Z} and E_{int} are the Zeeman energy of uncompensated AF moments and interfacial coupling energy, respectively. On the other hand, negative exchange bias (NEB), with the hysteresis loop shifted in the direction opposite to H_{FC} , arises when H_{FC} is smaller than the interfacial coupling, which aligns AF moments antiparallel with the field. The spontaneous reversal phenomenon observed in PEB systems implies $|E_{int}| > |E_{FM-Z}| + |E_{pinning}| > |E_{FM-Z}|$; therefore, $|E_{AF-Z}| > |E_{FM-Z}|$, or equivalently, $|m_{AF}| > |m_{FM}|$, where m_{FM} and m_{AF} are FM and uncompensated AF magnetic moments, respectively. However, experimentally, we find both the vertical shift of the low-temperature hysteresis loop and the change in saturation magnetization from $T=150$ to 10 K to be smaller than 2% of the saturation magnetization (i.e., within the measurement error).¹² Since the above two quan-

ties are signatures of pinned and unpinned AF moments, respectively,¹³ the experimental result suggests precisely the opposite of what we expect: $|m_{FM}| \gg |m_{AF}|$. Therefore, spontaneous magnetization reversal must be interpreted as energetically unfavorable within the existing framework of exchange bias. A lower energy state would have positive FM and negative AF moments, corresponding to negative rather than the observed positive EB. This contradiction implies that either spontaneous reversal is a novel metastable state or our present understanding of exchange bias is incomplete.

It has been proposed that AF or FM domain walls parallel to the interface are important for a complete picture of exchange bias.¹⁴⁻¹⁶ Experimentally, AF parallel domain walls have been observed by magnetometry,^{17,18} polarized neutron scattering,¹⁹ and x-ray magnetic linear dichroism.²⁰ FM parallel domain walls were observed by Kerr effect in accord with micromagnetic simulations.^{21,22} In addition, recent polarized neutron scattering experiments on samples similar to those displaying spontaneous reversal found negligible uncompensated AF moments in the bulk for NEB with $H_{FC}=0.1$ kOe, while nonzero bulk uncompensated AF moments were found for PEB with $H_{FC}=7$ kOe.²³ These neutron scattering results also suggest that the negative interfacial coupling leads to the formation of parallel domain walls in the FM for PEB samples.

This work reports on the dynamics and thermal training of spontaneous magnetization reversal and proposes an extended exchange bias model that accounts for the observed results by including the formation of parallel domain walls. We demonstrate experimentally that larger reversal magnitudes can be achieved by (a) low cooling rates, (b) long isothermal relaxation with $T \sim T_N$, and (c) successive thermal cycling about T_N . These results show that spontaneous magnetization reversal is energetically favored rather than metastable, as predicted by existing positive EB models. Modeling this system by explicitly taking into consideration the formation of domain walls parallel to the FM/AF interface in either the FM or the AF reveals that the sign of EB depends on the competition between the formation of these domain walls and the interfacial coupling. We show that the relevant competition may be tuned via the FM thickness, which leads to the prediction of the spontaneous reversal phenomenon and its observed dynamical behavior.

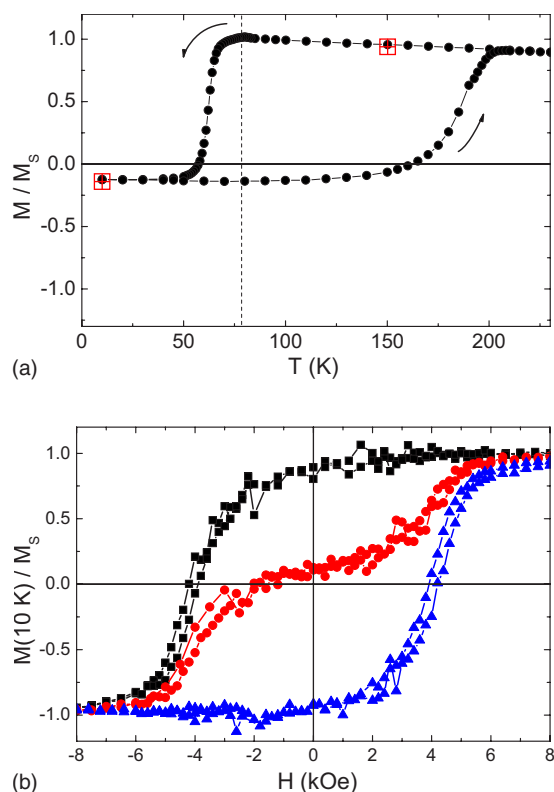


FIG. 1. (Color online) (a) M vs T of Ni/FeF₂ normalized by M_S with $H_{FC}=0.1$ kOe. The dashed line marks $T_N=78$ K. The red crossed squares mark the initial and final normalized magnetizations of the same cooling procedure from 150 to 10 K but without measurement at intermediate temperatures. (b) Magnetic hysteresis at $T=10$ K after cooling with H_{FC} of -0.1 kOe (black square), 0.1 kOe (red circle), and 1 kOe (blue triangle) at 10 K/min.

II. EXPERIMENT

The same Ni(3 nm)/FeF₂(30 nm) sample on a MgF₂ substrate was studied as in our previous work.⁹ FeF₂ is an AF with $T_N=78$ K and grows epitaxially untwinned in the (110) direction on MgF₂ (110) substrates.²⁴ The FM exhibits uniaxial anisotropy with the easy axis parallel to FeF₂ [001] (the spin axis of the AF). The magnetic field was always applied along the easy axis of the FM. Prior to cooling, the FM was saturated with a 5 kOe field, well above the coercive field $H_C=0.35$ kOe at $T=150$ K, then reduced to H_{FC} . Figure 1(a) shows the thermally induced magnetization reversal in $H_{FC}=0.1$ kOe. Hysteresis measurements at $T=10$ K find NEB for -0.25 kOe $\leq H_{FC} \leq -0.1$ kOe, PEB at $H_{FC} > 0.5$ kOe, and coexistence for -0.1 kOe $\leq H_{FC} \leq 0.5$ kOe [Fig. 1(b)]. $|H_{EB}|=3.9 \pm 0.1$ kOe for all cooling fields. Coexistence of PEB and NEB for an intermediate H_{FC} has been interpreted as the AF breaking into “domains” due to lateral inhomogeneity with uncompensated moments of either sign.^{24,25} When the lateral size of these domains is much larger than the FM domain wall width, they independently induce either PEB or NEB in the FM, causing the experimentally observed double hysteresis loop. Since only PEB is essential for spontaneous reversal, partial reversal was observed for intermediate H_{FC} with coexistent PEB and NEB [Fig. 1(a)].

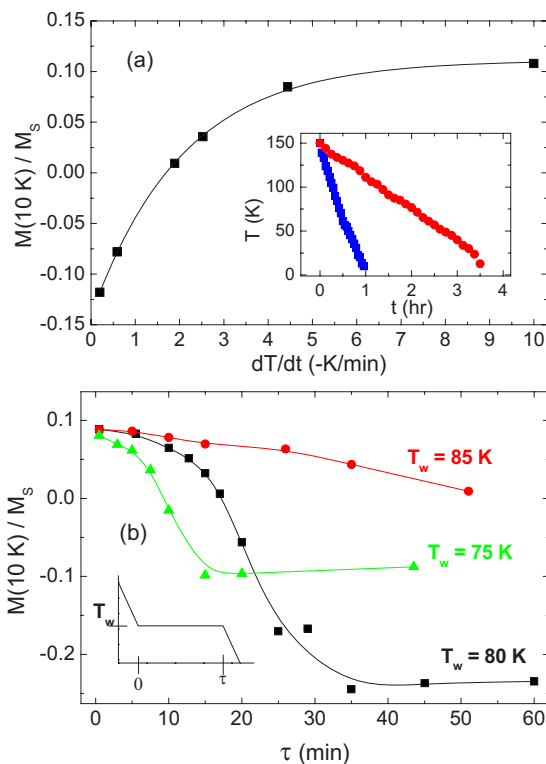


FIG. 2. (Color online) (a) M/M_S at $T=10$ K as a function of uniform cooling speed dT/dt for $H_{FC}=0.1$ kOe. The line is a fit to an exponential function. (Inset) Temperature vs time for uniform cooling speeds of 2.5 [blue (dark gray)] and 0.6 K/min [red (light gray)]. (b) M/M_S at $T=10$ K as a function of wait time τ at temperatures $T_w=75$ (green triangle), 80 (black square), and 85 (red circle) K for $H_{FC}=0.1$ kOe. (Inset) Schematic of this cooling protocol. Lines are a guide to the eyes.

Two different cooling protocols were used to investigate the time dependence of the reversal magnitude. We only consider $H_{FC}=0.1$ kOe, for which the magnetization reverses from saturation at $T=150$ K to $M \approx 0$ at $T=10$ K. In the first protocol, the sample was cooled from $T=150$ to 10 K with two decades (0.1 – 10 K/min) of uniform cooling speeds [Fig. 2(a) inset]. In the second protocol, the sample was cooled at 10 K/min from 150 K to an intermediate temperature T_w , where the temperature was held constant for a time τ , then decreased to 10 K at 10 K/min [Fig. 2(b) inset]. For both protocols, $M(T=10$ K) was measured after the sample temperature stabilized at 10 K.

Figure 2(a) shows that slower cooling leads to a larger reversal magnitude. After cooling to 10 K at the largest cooling speed of 10 K/min, the FM reverses from the positive saturation (M_S) to $0.11M_S$. When cooled at 0.1 K/min, it reverses from M_S to $-0.12M_S$. Moreover, the dependence of M at 10 K on the cooling speed is well fitted by an exponential function $M=M_0-A \exp(-\alpha dT/dt)$. This fit implies that the FM reverses to $M_0=-0.14M_S$ and $M_0-A=0.11M_S$ in the limits of zero and infinite cooling speeds, respectively.

The second cooling protocol demonstrates that the magnetization reversal is sensitive to the time spent at $T \sim T_N$. The dependence of the magnetization at $T=10$ K on the wait temperature T_w shows the largest reversal for $T_w=80$ K, clos-

est to T_N (Fig. 2). The magnetization at 10 K decreases from $0.09M_S$ with $\tau=0$ to $-0.23M_S$ with $\tau>35$ min. For $T_w=85$ K, M only changes by $0.07M_S$ after waiting for 50 min. For $T_w=75$ K, $M(T=10$ K) saturates after ~ 15 min at $-0.1M_S$. No wait-time dependence was observed when waiting at the reversal temperature ($T=63$ K). The results from these two cooling protocols show that spontaneous magnetization reversal exhibits slow dynamics with a time scale on the order of 10 min. The fact that the dynamics is most pronounced around T_N hints that this effect depends on the establishment of AF domains.

Slow evolution of the system toward a larger reversal implies the presence of large energy barriers. It has been shown that AF/FM exchange coupling can reorient AF moments at high temperatures, causing H_{EB} to exponentially decay with the wait time at a fixed temperature.^{26,27} The large uniaxial anisotropy of FeF_2 ($K=1.35 \times 10^4$ kJ/m³) gives rise to a large energy barrier for reversal of AF spins once the AF is ordered. Therefore, the wait-time dependence can only be observed at $T \approx T_N$ when the anisotropy is still small. The above experiment also suggests the presence of inhomogeneous AF grains so that uncompensated moments in some of them orient along or against the field direction regardless of the cooling protocol, and the orientation of the rest depends on the cooling details. This is consistent with the model of polycrystalline AF in the literature. Although FeF_2 in our sample is epitaxially grown, the inevitable inhomogeneity of the uniaxial anisotropy magnitude gives rise to an energy barrier distribution, and hence shows features similar to those previously observed in polycrystalline systems.²⁸ More about the importance of the in-plane inhomogeneity will be addressed later in the discussion. Below, we show that the system can be thermally trained and can overcome this energy barrier by cycling the temperature above and below T_N .

The sample was first cooled (with the FM saturated) in $H_{FC}=0.1$ kOe from 150 to 10 K at 0.1 K/min, followed by heating to 150 K, just below the temperature for the FM to reverse back along the field direction (Fig. 1). After that, the sample was cycled between 150 and 10 K. The magnetic field was held constant at $H_{FC}=0.1$ kOe throughout the thermal cycles. The FM reverses with each additional cooling (with decreasing incremental reversal magnitude) until the magnetization at $T=10$ K reaches $-0.8M_S$, significantly larger than the initial reversal for any cooling speed or wait time [Fig. 3(a)].

Figure 3(b) shows the dependence of $M(10$ K) on the number of cycles N for different H_{FC} and cooling speeds. For all cases, they follow an exponential dependence, $M_N(10$ K) = $M_\infty + (M_S - M_\infty)\exp(-N/\eta)$, where M_∞ is the convergent $M(10$ K) when N approaches infinity and η is a characteristic cycle number for each H_{FC} and cooling speed. $M_{N=0}$ is defined as M_S . M_∞ appears to be linearly dependent on H_{FC} for constant cooling speed [Fig. 3(b) inset]. Larger H_{FC} results in smaller η , which means a faster approach to M_∞ . This is reasonable because a larger magnetic field should facilitate reversal by lowering the energy barrier so that more AF moments may align with H_{FC} .

Several tests were performed to ensure that the observed dynamics were not experimental artifacts, such as magnetic

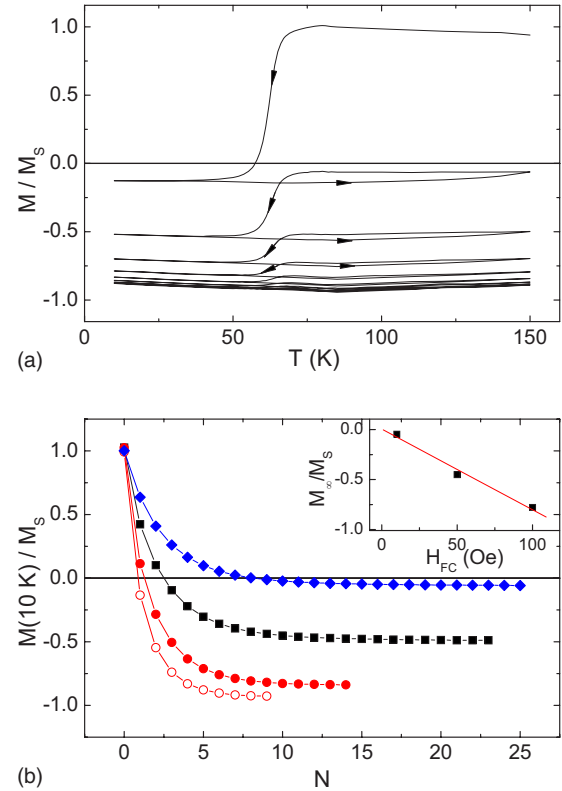


FIG. 3. (Color online) (a) Normalized magnetization M/M_S was measured as the temperature was cycled between 150 and 10 K in a 0.1 kOe field. Nine cycles were conducted. (b) Normalized magnetization M/M_S at $T=10$ K after each thermal cycle between 150 and 10 K as a function of the number of cycles, N . Different cooling parameters were used, $H_{FC}=10$ Oe (blue diamond), 50 Oe (black square), and 100 Oe (red filled circle) with 10 K/min cooling and heating rates, and $H_{FC}=100$ Oe with 0.1 K/min (red empty circle). The lines are a guide to the eyes. (Inset) Asymptotic magnetization M_∞/M_S at high cycling number N obtained by exponential fitting as a function of H_{FC} . The red line is a linear fit.

field inhomogeneity or temperature fluctuation. To exclude the artifact of magnetic field inhomogeneity when moving the sample through the superconducting quantum interference device (SQUID) coil by 4 cm, the cooling procedure used to obtain the data of Fig. 1 was repeated but measuring only the initial and final magnetization values rather than at several intermediate temperatures. The sample was thus only exposed to field inhomogeneity at these extreme temperatures. The reversal magnitude only differs by $3 \times 10^{-4}M_S$ between these two methods, which is negligibly small. To investigate the influence of temperature fluctuation during sample cooling and temperature stabilization, the sample was cycled between 10 K and T_x . When $T_x=150$ K, this corresponds to the earlier experiments investigating thermal training (Fig. 3). When $T_x \leq 80$ K, the reversal magnitude varies by no more than $0.01M_S$, too small to account for the time dependence found earlier (Fig. 4). When $T_x > 80$ K, a significant additional magnetization reversal was observed, and its magnitude is the same as that corresponding to $N=2$ on the red curve in Fig. 3(a). These checks demonstrate that the time sensitivity of spontaneous reversal is not an experimen-

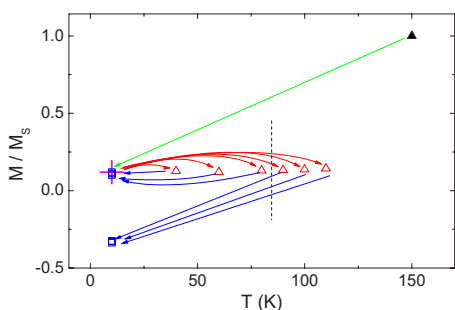


FIG. 4. (Color online) Normalized magnetization M/M_S was measured after each step of the three-step thermal cycle: (1) cooling from $T=150$ to 10 K (magenta cross); (2) warming to T_x (40–110 K) (red triangles); (3) cooling back down to 10 K (blue squares). M/M_S was reversible for $T_x < 80$ K but irreversible above 80 K. The dashed line separates these two regimes and is close to T_N . The lines are schematics of the measurement sequence.

tal artifact but rather is intrinsic to the system and unambiguously related to the AF phase transition. Larger reversal for slower cooling rates and longer wait times around T_N suggests that spontaneous reversal is thermodynamically favorable.

III. EXTENDED EXCHANGE BIAS MODEL

These experiments suggest that it is energetically favorable for the FM to reverse against H_{FC} , albeit counterintuitive since $|m_{FM}| \gg |m_{AF}|$. This behavior cannot be explained simply by the competition between the Zeeman energy and interfacial coupling. Although the inhomogeneity of AF grains plays an important role²⁸ in the dynamic process, as will be addressed below, the fact that these AF grains have spatially variant AF moments cannot resolve the contradiction because the total uncompensated AF moments are much smaller than FM moments and thus cannot lead to spontaneous FM reversal. An additional controversy arises from the values of H_{FC} required for establishing PEB. Consider that $[M_S - M(10\text{ K})]/2M_S$ gives the percentage of sample that exhibits PEB at 10 K for an intermediate H_{FC} . For $H_{FC} = 0.1$ kOe, the sample is nearly 90% positively exchange biased at 10 K after six thermal cycles at 0.1 K/min. The interfacial coupling energy in this sample is $E_{int} = J_{FM/AF} \mathbf{S}_{FM} \cdot \mathbf{S}_{AF} = \mu_0 H_{EB} M_{FM} t_{FM} = 0.79$ erg/cm², close to that previously found in similar systems.²⁹ However, the onset H_{FC} for PEB in this case is about 2 orders of magnitude smaller than that previously found.³⁰ This very small H_{FC} necessary for PEB challenges present interpretations of PEB and implies the necessity of a model that can explain our observation.

Here, we propose an extended model of exchange bias that can explain both the sign of exchange bias being tuned by the cooling field and the occurrence of spontaneous magnetization reversal. Based on recent experimental results and exchange bias models,^{14–16,20,22,23,31} our model explicitly considers the parallel domain wall energy in either the ferromagnet or antiferromagnet. In the case of NEB, a parallel domain wall is developed in the AF. In contrast, PEB results

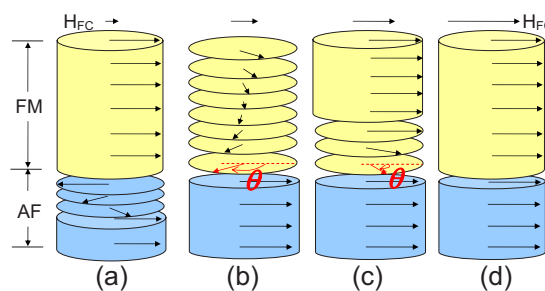


FIG. 5. (Color online) Schematic spin structures for NEB and PEB with H_{FC} to the right. The arrows are net uncompensated moments in the AF and local magnetization in the FM. (a) For NEB, a 180° parallel domain wall forms in the AF near the interface, with bulk AF moments positive. For PEB, three scenarios arise: (b) an incomplete parallel domain wall spans the entire FM thickness; (c) a parallel domain wall forms near the FM/AF interface with the topmost FM moments positively saturated; (d) the entire FM is saturated.

from either a parallel domain wall in the FM or a fully saturated FM that frustrates the interfacial coupling for sufficiently large H_{FC} . By minimizing the total system energy, we are able to determine the ground state spin configuration with increasing cooling fields, and hence the onset cooling field for PEB. When the FM thickness is small compared to its domain wall width, small cooling fields are sufficient to establish PEB and spontaneous reversal. Moreover, with decreasing temperatures, PEB is increasingly energetically favored over NEB. Slow cooling or longer waiting around T_N increases the probability of reorienting AF moments and therefore increasing the magnetization reversal magnitude.

A. Model details

Based on the above experimental observations, we make the following important assumptions in our model. (i) The FM and AF are assumed to be separated by a sharp interface. (ii) The magnitude of uncompensated interfacial AF moments is assumed constant, regardless of its sign, because the absolute value of H_{EB} is found to be independent of its sign.^{9,24,25} (iii) Uncompensated AF spins are taken to be ferromagnetically coupled among themselves, but antiferromagnetically coupled to FM spins. (iv) When a parallel domain wall is formed in the AF near the interface, the AF thickness is assumed to be large enough to contain a full 180° AF domain wall. This is a reasonable assumption considering the large uniaxial anisotropy of the AF, and therefore a small domain wall width (1–3 nm).³² (v) Based on recent neutron scattering results,²³ uncompensated moments in the bulk of the AF are assumed to align positively, and their magnitude is proportional to H_{FC} for simplicity. As suggested by the spontaneous magnetization reversal experiment,⁹ the Zeeman energy of bulk AF moments is much smaller than both that of FM moments and the interfacial coupling, and is thus ignored.

Figure 5 qualitatively depicts the spin structures used in our model after field cooling in H_{FC} . For either sign of exchange bias, bulk AF and FM moments (those far from the

interface) are favored to align with the cooling field. Competition of the magnetic field and the antiferromagnetic interfacial coupling leads to frustration of the spins at the interface. This frustration results in a parallel domain wall in either the FM or AF, depending on the relevant energies. It is worth noting that uncompensated moments in the bulk of the AF play a critical role in this model. These AF moments form a parallel domain wall with those at the interface in the case of NEB, and their magnitude determines the domain wall energy in the AF in competition with that in the FM. This is consistent with the idea of domain state model, where the bulk AF moments arising from dilution of impurity or defects lead to AF domain structures crucial to the understanding of exchange bias.³¹ However, in our model, the domain structure in the FM is equally important as that in the AF, and as we will show next, the domain wall energy of the FM can dominate over that of the AF and give rise to spontaneous magnetization reversal or rotation.

NEB is typically observed for small H_{FC} . In this case, the FM aligns with H_{FC} , and the antiferromagnetic interfacial coupling causes the interfacial AF moments to orient against the field. Since both the magnetic field and the interfacial coupling favor the FM parallel to H_{FC} , the FM is uniformly saturated in the field direction, as shown in Fig. 5(a). However, a parallel domain wall is formed between positive bulk and negative interfacial AF moments. This parallel AF domain wall is similar to what was proposed by Mauri *et al.*,¹⁴ but here, it freezes upon cooling and does not respond to a changing magnetic field. Because of the large uniaxial anisotropy of the AF, the energy cost for establishing NEB arises mainly from the parallel AF domain wall formation.

For PEB, typically established with a large H_{FC} ,⁶ both interfacial and bulk AF moments are positively aligned. In this case, since the AF interfacial coupling favors FM moments to align opposite to the field, three FM domain structures may result depending on H_{FC} , the FM thickness, domain wall width, and interfacial coupling. When H_{FC} is relatively small (but large enough for PEB) and the FM is thinner than the FM domain wall width, an incomplete parallel domain wall spans the entire FM thickness [Fig. 5(b)]. With increasing H_{FC} , FM moments will be twisted toward the field direction until the top of the FM is aligned with H_{FC} , with the incomplete domain wall compressed near the FM/AF interface [Fig. 5(c)]. In these two cases, the energy cost is on forming the incomplete parallel FM domain wall and frustrating the interfacial coupling. A large enough H_{FC} may also fully saturate the FM, hence eliminating the parallel domain wall [Fig. 5(d)]. This configuration is a special case of that shown in Fig. 5(c) for $\theta=0$, where θ is the angle between interfacial FM moments and H_{FC} (Fig. 5). In this situation, the energy cost is only on frustrating the interfacial coupling.

First, we consider the system energies for NEB and PEB at $T=0$ K. The nonzero temperature scenario will be evaluated phenomenologically in the discussion of the dynamics of spontaneous magnetization reversal. In general, the system energies for NEB and PEB can be formulated as

$$E_{NEB} = E_{FM-Z} + E_{AF-Z} + E_{int} + E_{AF-DW},$$

$$E_{PEB} = E_{FM-Z} + E_{AF-Z} + E_{int} + E_{FM-DW},$$

where E_{FM-Z} , E_{AF-Z} , and E_{int} are the FM Zeeman, AF Zeeman, and interfacial coupling energies, respectively. For NEB, due to lack of knowledge of the details of the functional form of bulk uncompensated AF moments vs cooling field, it is not possible to quantitatively evaluate E_{NEB} . However, assuming a linear dependence of bulk AF moments on H_{FC} and the energy cost to form the AF domain wall proportional to the bulk AF moments, the AF domain wall energy can be written as $E_{AF-DW} = \alpha H_{FC}$. The importance of the sample-dependent coefficient α is qualitatively illustrated in Sec. III B, and an estimate of α is given in the discussion. Assuming E_{AF-Z} to be negligible, as previously noted, the system energy can be formulated as

$$E_{NEB} \approx -H_{FC}M_{FM}t_{FM} + 0 + E_{int0} + \alpha H_{FC} = E_0 + \alpha H_{FC},$$

where $E_0 = -H_{FC}M_{FM}t_{FM} - E_{int0}$ is a reference energy for comparison with PEB, where $E_{int0} < 0$ is the minimum interfacial coupling energy with antiparallel interfacial moments S_{FM} and S_{AF} and negative interfacial coupling J_{FM-AF} .

For PEB, we define a reduced FM thickness $t = t_{FM} / \delta_{DW}$, where δ_{DW} is the FM domain wall width. For the case of an incomplete FM domain wall as in Fig. 5(b) [$t_{FM} < (\theta/\pi)\delta_{DW}$, or $t < \theta/\pi$], the system energy is

$$E_{PEB1} = E_0 + H_{FC}M_{FM}\delta_{DW} \frac{[t\pi - \sin\theta + \sin(\theta - t\pi)]}{\pi} + E_{int0}(\cos\theta + 1) + t\pi\sqrt{A_{FM}K_{FM}},$$

For the case of Figs. 5(c) and 5(d) ($t \geq \theta/\pi$),

$$E_{PEB2} = E_0 + H_{FC}M_{FM}\delta_{DW}(\theta - \sin\theta)/\pi + E_{int0}(\cos\theta + 1) + \theta\sqrt{A_{FM}K_{FM}}.$$

Minimizing E_{PEB} with respect to θ gives the energetically favorable spin structure for each H_{FC} at $T=0$ K.

It is convenient to define a reduced energy $\mathcal{E} = (E - E_0) / |E_{int0}|$ and a reduced cooling field $h_{FC} = H_{FC} / H_{EB0}$, where H_{EB0} is the exchange bias field when $t_{FM} = \delta_{DW}$, assuming the inverse thickness dependence of H_{EB} according to the Meiklejohn-Bean model.¹ In this convention, the reduced exchange bias field for a reduced thickness $t = t_{FM} / \delta_{DW}$ is $h_{EB} = H_{EB} / H_{EB0} = \delta_{DW} / t_{FM} = 1/t$. Using the experimentally determined parameters in the previous section, we find $E_{int0} = -\mu_0 M_{FM} |H_{EB}| t_{FM} = -7.9 \times 10^{-4}$ J/m². Using a Ni exchange stiffness $A_{FM} = 3.4$ pJ/m and anisotropy $K_{FM} = 5$ kJ/m³, the areal energy density of a FM domain wall spanning 1 rad is $\sqrt{A_{FM}K_{FM}} = 1.30 \times 10^{-4}$ J/m². The reduced system energies for PEB using these parameters is plotted in Fig. 6(a) for several reduced thicknesses.

B. Model results

This model predicts the existence of PEB with onset cooling fields much smaller than H_{EB} , and thus spontaneous magnetization reversal. The intersection of the PEB and NEB system energies in Fig. 6(a) gives the cooling field h_{FC}^0 for PEB onset. Varying the linear coefficient α in E_{NEB} can

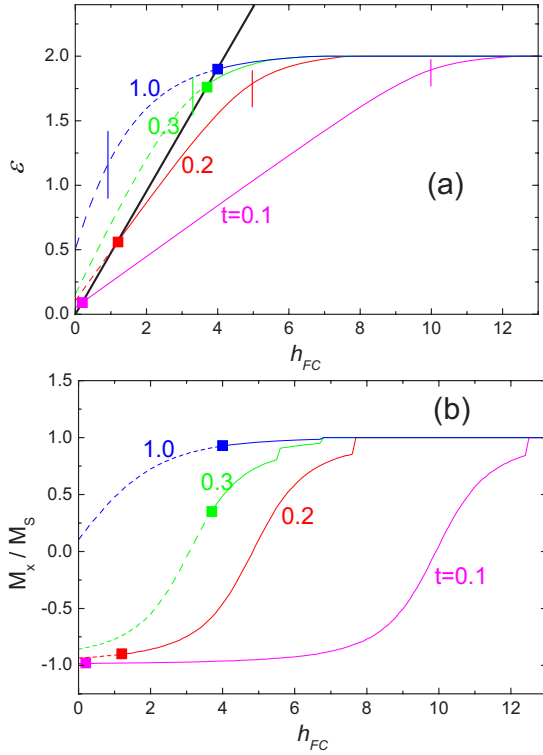


FIG. 6. (Color online) (a) Reduced system energy \mathcal{E} for NEB (thick black line) and PEB (other curves) as a function of h_{FC} for $t=t_{FM}/\delta_{FM}=0.1$ (magenta), 0.2 (red), 0.3 (green), and 1.0 (blue). Square data points mark the onset h_{FC} for PEB, below which NEB is energetically favored and \mathcal{E}_{PEB} are shown as dashed lines. Vertical lines mark the reduced exchange bias field $h_{EB}=1/t$ for different FM thicknesses. (b) FM magnetization M_x along H_{FC} normalized by saturation magnetization M_S as a function of h_{FC} .

change the intersection of E_{NEB} and E_{PEB} , and hence h_{FC}^0 . Moreover, a larger α leads to smaller h_{FC}^0 . Figure 6(a) shows a possible scenario that demonstrates PEB and predicts spontaneous magnetization reversal. The magnetization along the cooling field, M_x , is plotted in Fig. 6(b) for the case of PEB, which shows that both spontaneous magnetization reversal and rotation are predicted by this model and are thus energetically favored.

h_{FC}^0 for PEB decreases with decreasing FM thickness. When $t=0.1$ ($t_{FM}=8$ nm for Ni), Fig. 6(a) shows that very small $h_{FC} \geq 0.1$ is sufficient for PEB. The FM magnetization aligns antiparallel with h_{FC} until h_{FC} is larger than ~ 8 , still smaller than $h_{EB}=10$. It is worth noting that the condition for thermally induced magnetization reversal is that h_{FC} for PEB is smaller than h_{EB} with small FM uniaxial anisotropy.⁹ With increasing t , h_{FC}^0 increases, h_{EB} decreases, and the range of h_{FC} where spontaneous reversal is possible decreases. When $t \geq 0.3$ ($t_{FM}=24$ nm for Ni), h_{EB} becomes smaller than h_{FC}^0 , and full reversal is not found. However, applying h_{FC}^0 just large enough to induce PEB with $t=0.3$ orients the interfacial FM moments at 96° relative to h_{FC} , and $M_x/M_S=0.35$. This suggests spontaneous FM rotation and an incomplete FM parallel domain wall. This was found experimentally in previous vector SQUID measurements of a similar sample but with 21 nm thick Ni, whose thickness is about 25% of its

domain wall width.⁹ Interestingly, for $t=1$, the interfacial FM moments orient at $\theta=62^\circ$ even when $h_{FC} \sim 4$, much larger than $h_{EB}=1$, even though the total FM magnetization is almost fully aligned with the field ($M_x/M_S=0.93$). This suggests that parallel FM domain walls persist for magnetic fields much larger than H_{EB} , which is consistent with previous findings.²² For all thicknesses and large enough h_{FC} , the FM is fully positively saturated, which corresponds to the commonly observed and generally assumed minimum-energy state.

This model also allows insight into the origin of the dynamics of spontaneous reversal, which we attribute to the change of the system ground state with temperature. As the temperature decreases below T_N , the AF starts ordering with increasing uncompensated AF moments and H_{EB} .² As demonstrated below, temperature can be phenomenologically incorporated into our model via interfacial coupling E_{int} or H_{EB} : decreasing temperature corresponds to increasing H_{EB} and vice versa.

Figure 7(a) shows the model results for $t=0.1$ with $H_{EB}=0.1, 0.2,$ and 4 kOe, in real units of H_{FC} . The dependence of the PEB onset cooling field H_{FC}^0 on H_{EB} is shown in Fig. 7(b). When T is just below T_N with H_{EB} as small as 0.1 kOe [solid red line in Fig. 7(a)], the FM is always fully saturated regardless of $|H_{FC}|$, which corresponds to the spin configuration in Fig. 5(d) and $\mathcal{E}_{PEB}=2$. In this case, the sign of EB is only determined by the competition of the AF domain wall energy with the interfacial coupling and is independent of t_{FM} . Since NEB was not observed for $H_{FC} \geq 0.5$ kOe, the linear coefficient α of the NEB system energy is chosen so that the NEB and PEB system energies intersect at $H_{FC}=0.5$ kOe, as marked by the red square in Fig. 7(a). This yields $\mathcal{E}_{NEB}=4$ kOe⁻¹ H_{FC} . With decreasing T and thus increasing H_{EB} , H_{FC}^0 decreases due to the possibility of forming a parallel domain wall in the FM with increasing interfacial coupling, as shown in Fig. 7(b). The lowest H_{FC}^0 for PEB is found when the maximum H_{EB} is reached (4 kOe, solid blue line), as marked in Fig. 7(a) with the blue square. The red and blue dashed lines in Fig. 7(a) indicate the bounds of H_{FC} , above (below) which only PEB (NEB) will be favored for all temperatures. For H_{FC} between these bounds, NEB becomes increasingly unfavorable with decreasing temperature (increasing H_{EB}).

IV. DISCUSSION

With this extended model of exchange bias, we are able to interpret the experiments presented earlier. In real systems, the AF layer can be considered as an ensemble of AF grains with spatially inhomogeneous magnetic properties,^{28,33} e.g., interfacial coupling. This leads to a distribution of H_{FC}^0 , which is evidenced by the large range of cooling fields that yield the coexistence of PEB and NEB.^{24,25} This also results to broadening of the boundaries in Fig. 7(a) (two dashed lines) into a continuous field range. When the sample is cooled with H_{FC} contained within the broadened boundary, some areas of the sample will always favor one sign of exchange bias, regardless of temperature. For example, if H_{FC} is within the broadened boundary, some areas of the sample

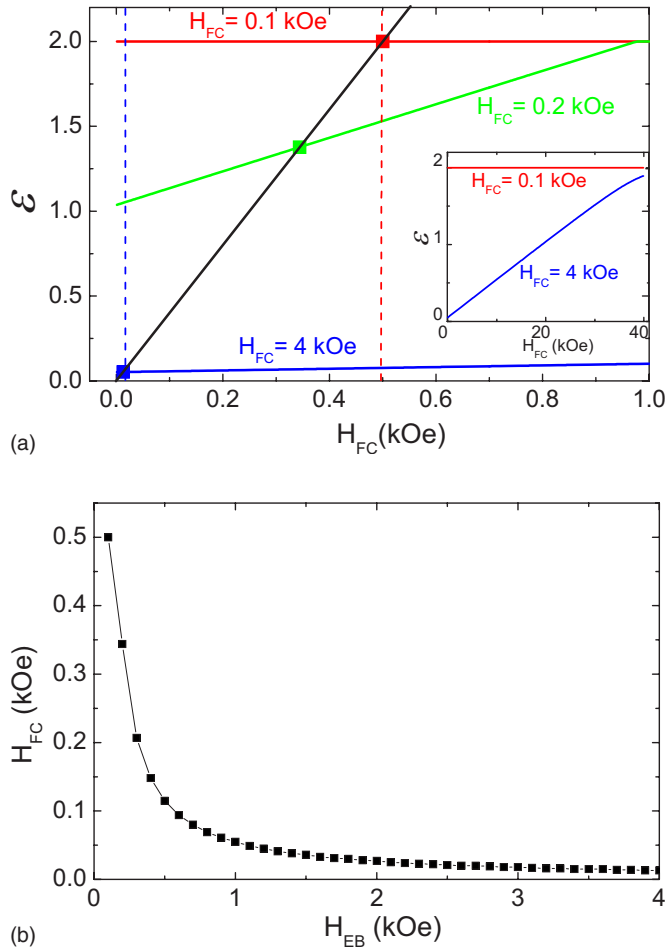


FIG. 7. (Color online) (a) Reduced energy \mathcal{E} as a function H_{FC} for NEB (black line) and PEB for $t=0.1$ when $H_{EB}=0.1$ (red), 0.2 (green), 4 kOe (blue). The left and right dashed lines mark the cooling fields above which PEB is favored for $H_{EB}=4$ and 0.1 kOe, respectively. The square symbols mark the onset H_{FC} for PEB. (Inset) Zoom-out of PEB energies for PEB when $H_{EB}=0.1$ (red), 4 kOe (blue). (b) Calculated onset H_{FC} for PEB as a function of H_{EB} .

will always show NEB because H_{FC} is below the local lower boundary. Elsewhere on the sample, NEB is only favored for small HEB just below T_N . As H_{EB} increases with decreasing temperature, NEB becomes energetically unfavored in these regions, and AF moments tend to reverse their sign to favor PEB.

The time scale of reversing AF moments depends on the temperature and corresponding anisotropy barrier. If the temperature at which NEB becomes unfavored is close to T_N , the anisotropy energy is small enough³⁴ for thermal fluctuations to realign the uncompensated AF moments in the positive direction. This causes the fraction of the sample exhibiting PEB to grow. This growth is a thermodynamic process with an increasing probability of local switching of the exchange bias sign with slower cooling or longer waiting around T_N . This gives rise to the time dependence of the reversal magnitude presented in Fig. 2. The large anisotropy barrier results in the long reversal time scales.

When the temperature at which NEB becomes unfavored is much lower than T_N , AF moments are already frozen and

the system will not be able to reach its ground state with a single cooling event. However, it is possible to reach the ground state via thermal training. It is worth noting that the thermal training occurs with the magnetic field fixed at H_{FC} . After the first cooling, the FM and AF moments are aligned negatively (positively) and positively (negatively), respectively, in the positive (negative) biased region of the sample. However, due to the much larger domain wall width of the FM than that of the AF, FM moments vary from positive to negative orientation over a much larger lateral length scale than the AF. Warming the sample above T_N frees AF spins while the FM domain state is unchanged. Since the FM spins composing lateral domain walls are not fully positive (as they were prior to the first cooling), the energy cost in establishing PEB, or the interfacial coupling [the $H_{EB}=0.1$ kOe horizontal line in Fig. 7(a)], becomes smaller than in the first cooling at $T \sim T_N$. Therefore, it becomes easier to orient in the AF spins that lie beneath the FM domain wall in the positive direction, thereby promoting PEB. In this way, the fraction of the sample displaying PEB expands at the cost of the NEB region, which causes the magnitude of the magnetization reversal to increase incrementally with each thermal cycle. This process repeats itself successively until the low-temperature system ground state is finally reached.

V. CONCLUSIONS

In summary, different cooling protocols revealed that spontaneous magnetization reversal in exchange biased heterostructures leads to the energy ground state, not a metastable state implied by existing exchange bias models. Slower cooling speeds and isothermal relaxation around T_N lead to larger magnetization reversal. Thermal training was discovered by cycling the sample temperature about T_N , causing the FM to reverse successively with each cycle, reflecting the incremental conversion of negatively exchange biased regions to positively biased ones. An extended model of exchange bias that predicts spontaneous reversal and slow dynamics by considering the energy stored in antiferromagnetic and ferromagnetic parallel domain walls is presented. Further, this model shows that negative exchange bias arises when a parallel antiferromagnet domain wall is developed between the uncompensated interfacial and bulk antiferromagnet moments, while positive exchange bias occurs when parallel FM domains develop and frustrate interfacial coupling. Accounting for this parallel domain wall energy resolves the contradiction of present positive exchange bias models with the existence of thermally induced spontaneous magnetization reversal.

ACKNOWLEDGMENTS

This work was supported by U.S. DOE. The authors thank R. Victora, T. Gredig, and R. Morales for illuminating discussions.

- *Present address: Center for Nanoscale Systems, Cornell University, Ithaca, NY 14853; z165@cornell.edu
- †Permanent address: Physics Department, University of South Florida, Tampa, FL 33620.
- ‡Also at: Physics Department, Texas A&M University, College Station, TX 77843.
- ¹W. H. Meiklejohn and C. P. Bean, *Phys. Rev.* **105**, 904 (1957).
- ²J. Nogués and I. K. Schuller, *J. Magn. Magn. Mater.* **192**, 203 (1999).
- ³M. Kiwi, *J. Magn. Magn. Mater.* **234**, 584 (2001).
- ⁴J. C. S. Kools, *IEEE Trans. Magn.* **32**, 3165 (1996).
- ⁵V. Skumryev, S. Stoyanov, Y. Zhang, G. Hadjipanayis, D. Givord, and J. Nogués, *Nature (London)* **423**, 850 (2003).
- ⁶J. Nogués, D. Lederman, T. J. Moran, and I. K. Schuller, *Phys. Rev. Lett.* **76**, 4624 (1996).
- ⁷D. Paccard, C. Schlenker, O. Massenet, R. Montmory, and A. Yelon, *Phys. Status Solidi* **16**, 301 (1966).
- ⁸A. Hoffmann, *Phys. Rev. Lett.* **93**, 097203 (2004).
- ⁹Z.-P. Li, J. Eisenmenger, C. W. Miller, and I. K. Schuller, *Phys. Rev. Lett.* **96**, 137201 (2006).
- ¹⁰E. L. Venturini and P. M. Richards, *J. Appl. Phys.* **47**, 1632 (1976).
- ¹¹S. Demirtas, M. R. Hossu, R. E. Camley, H. C. Mireles, and A. R. Koymen, *Phys. Rev. B* **72**, 184433 (2005).
- ¹²The quantities are obtained from the measurement of magnetic hysteresis with positive and negative exchange biases shown in Fig. 1(b).
- ¹³J. Nogués, C. Leighton, and I. K. Schuller, *Phys. Rev. B* **61**, 1315 (2000).
- ¹⁴D. Mauri, H. C. Siegmann, P. S. Bagus, and E. Kay, *J. Appl. Phys.* **62**, 3047 (1987).
- ¹⁵M. Kiwi, J. Mejía-López, R. D. Portugal, and R. Ramírez, *Appl. Phys. Lett.* **75**, 3995 (1999).
- ¹⁶N. C. Koon, *Phys. Rev. Lett.* **78**, 4865 (1997).
- ¹⁷S. Urazhdin and C. L. Chien, *Phys. Rev. B* **71**, 220410(R) (2005).
- ¹⁸C. L. Chien, V. S. Gornakov, V. I. Nikitenko, A. J. Shapiro, and R. D. Shull, *Phys. Rev. B* **68**, 014418 (2003).
- ¹⁹S. Roy, M. R. Fitzsimmons, S. Park, M. Dorn, O. Petravic, I. V. Roshchin, Z.-P. Li, X. Battle, R. Morales, A. Misra, X. Zhang, K. Chesnel, J. B. Kortright, S. R. Sinha, and I. K. Schuller, *Phys. Rev. Lett.* **95**, 047201 (2005).
- ²⁰A. Scholl, M. Liberati, E. Arenholz, H. Ohldag, and J. Stöhr, *Phys. Rev. Lett.* **92**, 247201 (2004).
- ²¹R. Morales, Z.-P. Li, O. Petravic, X. Battle, I. K. Schuller, J. Olamit, and K. Liu, *Appl. Phys. Lett.* **89**, 072504 (2006).
- ²²Z.-P. Li, O. Petravic, R. Morales, J. Olamit, X. Battle, K. Liu, and I. K. Schuller, *Phys. Rev. Lett.* **96**, 217205 (2006).
- ²³M. R. Fitzsimmons, B. J. Kirby, S. Roy, Z.-P. Li, I. V. Roshchin, S. K. Sinha, and I. K. Schuller, *Phys. Rev. B* **75**, 214412 (2007).
- ²⁴O. Petravic, Z.-P. Li, I. V. Roshchin, M. Viret, R. Morales, X. Battle, and I. K. Schuller, *Appl. Phys. Lett.* **87**, 222509 (2005).
- ²⁵I. V. Roshchin, O. Petravic, R. Morales, Z.-P. Li, X. Battle, and I. K. Schuller, *Europhys. Lett.* **71**, 297 (2005).
- ²⁶P. A. A. van der Heijden, T. F. M. M. Maas, W. J. M. de Jonge, J. C. S. Kools, F. Roozeboom, and P. J. van der Zaag, *Appl. Phys. Lett.* **72**, 492 (1998).
- ²⁷P. A. A. van der Heijden, T. F. M. M. Maas, J. C. S. Kools, F. Roozeboom, P. J. van der Zaag, and W. J. M. de Jonge, *J. Appl. Phys.* **83**, 7207 (1998).
- ²⁸J. Saha and R. H. Victora, *Phys. Rev. B* **73**, 104433 (2006).
- ²⁹J. Nogués, D. Lederman, T. J. Moran, I. K. Schuller, and K. V. Rao, *Appl. Phys. Lett.* **68**, 3186 (1996).
- ³⁰C. Leighton, J. Nogués, H. Suhl, and I. K. Schuller, *Phys. Rev. B* **60**, 12837 (1999).
- ³¹U. Nowak, K. D. Usadel, J. Keller, P. Miltényi, B. Beschoten, and G. Güntherodt, *Phys. Rev. B* **66**, 014430 (2002).
- ³²The Bloch domain wall width in bulk FeF₂ is 1 nm [M. T. Hutchings, B. D. Rainford, and H. J. Guggenheim, *J. Phys. C* **3**, 307 (1970)]. Using the anisotropy of the interfacial layer obtained in Roy *et al.* [*Phys. Rev. Lett.* **95**, 047201 (2006)], the domain wall width is about 3 nm.
- ³³E. Fulcomer and S. H. Charap, *J. Appl. Phys.* **43**, 4190 (1972).
- ³⁴H. Kondoh, *J. Phys. Soc. Jpn.* **15**, 1070 (1960).